Effective thermal conductivity of rough spherical packed beds

Majid Bahrami *, M. Michael Yovanovich, J. Richard Culham

Microelectronics Heat Transfer Laboratory, Department of Mechanical Engineering, University of Waterloo, Waterloo, ON, Canada N2L 3G1

Abstract

A new model is developed for predicting the effective thermal conductivity of regularly packed beds of rough, uniformly sized spheres immersed in a stagnant gas. Contact mechanics and thermal analyses are performed and the results are presented in the form of compact relationships. The present model accounts for the thermophysical properties of spheres and the gas, load, the rarefaction effects of the interstitial gas, gas temperature and pressure, and spheres diameter, roughness and asperities slope. The present model is compared with experimental data with the sphere diameter of 19.05, 25, and 50.4 mm and good agreement is observed.
© 2006 Elsevier Ltd. All rights reserved.

1. Introduction

Packed beds have a variety of applications in thermal systems. One of the significant characteristics of packed beds is the high ratio of solid surface area to volume. This property is useful in applications such as catalytic reactors, heat recovery processes, heat exchangers, heat storage systems, the breeder blanket about fusion reactors [1], and insulators. The insulator packed beds are often immersed in an stagnant gas at reduced pressure.

The thermal conductivity of packed beds is not isotropic. It is thus difficult to formulate a model that fully defines their effective thermal conductivity. However, the structure of a packed bed can be modeled assuming regular packing. A regularly packed bed is one in which the same arrangement of spheres (or cylinders), uniform in size, is repeated throughout the bed. Therefore, a typical "basic cell" can represent the entire regular bed. There are three such regular packings usually considered for packed beds:

(1) simple cubic (SC), (2) body center cubic (BCC), and (3) face center cubic (FCC). Tien and Vafai [2] showed that the FCC and SC packings present upper and lower bounds for the effective thermal conductivity of a random packed bed filled by a single phase fluid, respectively. Therefore, in this study the thermal conductivity of the SC and FCC arrangements are studied. The trends of the regularly packed beds (bounds) can be used to study the effect of important parameters involved in real (random) packed beds.

Many studies have been performed on the prediction of thermal conductivity of packed beds filled with a stagnant gas. The existing models can be categorized into two main groups. The first is numerical models, e.g., finite element methods (FEM) which can treat the three-dimensional problem by dividing the bed into many cells with temperature and heat flow matched at their boundaries. It is a combined thermal and mechanical three-dimensional numerical analysis which makes the FEM modeling extremely expensive from the calculative point of view [3]. In addition, thermal contact resistance (TCR) of rough spheres must be fed into the software as boundary conditions when commercial FEM software is used, thus the TCR problem must be solved separately. Buonanno and Carotenuto [4] used a three-dimensional FEM model to evaluate the thermal

---

* Corresponding author. Tel.: +1 519 888 4567x6181; fax: +1 519 746 9141.

E-mail addresses: majid@mhtlab.uwaterloo.ca (M. Bahrami), mmyov@mhtlab.uwaterloo.ca (M.M. Yovanovich), rix@mhtlab.uwaterloo.ca (J.R. Culham).

Nomenclature

A	area, m^2	ε	solid volume ratio, $\equiv V_s/V$
a_L	radius of macrocontact, m	γ	exponent of general pressure distribution
a_H	radius of Hertzian contact, m	γ_g	ratio of gas specific heats, $\equiv c_p/c_v$
b_L	chord of macrogap, m	Λ	mean free path, m
c_1	Vickers microhardness coefficient, Pa	κ	non-dimensional parameter, $\equiv \rho/a_H$
c_2	Vickers microhardness coefficient	υ	Poisson's ratio
D	sphere diameter, m	ξ	non-dimensional radial position, $\equiv r/a_L$
E	Young's modulus, Pa	ρ	radius of sphere, m
E'	effective elastic modulus, Pa	σ	RMS surface roughness, m
F	normal contact force, N	σ'	σ/σ_0, $\sigma_0 = 1$ μm
FCC	face center cubic	ω_0	bulk normal deformation at origin, m
H^*	$c_1(\sigma'/m)^{c_2}$, Pa		
Kn	Knudsen number	*Subscripts*	
k	thermal conductivity, W/m K	0	reference value, value at origin
L	length, m	1, 2	solid 1, 2
M	gas parameter, m	a	apparent
m	mean absolute surface slope	BR	boundary resistance
P	pressure, Pa	c	cell
Pr	Prandtl number	e	effective
Q	heat flow rate, W	g	gas, microgap
q	heat flux, W/m^2	G	macrogap
R	thermal resistance, K/W	H	Hertz
SC	simple cubic	j	joint
T	temperature, K	L	large, macrocontact
		r	real
Greek symbols		s	solid, micro
α	non-dimensional parameter, $\equiv \sigma\rho/a_H^2$		
α_T	thermal accommodation coefficient		

conductivity of simple cubic and body centered cubic packed beds and compared their model with experimental data collected by others. Buonanno et al. [3,5] conducted experiments and measured the effective thermal conductivity of uniformly sized rough stainless steel spheres. They compared their experimental data with their FEM numerical model and showed good agreement with the data. However, Buonanno et al. [3] did not report any expression or relationship for predicting the thermal conductivity of packed beds. Additionally, they did not compare their model with any data at reduced gas pressures.

The second group of existing models is the analytical models. These models break the problem into distinct conduction paths, e.g., the contact area between spheres, the gas layer between spheres, etc. The conductivity of the bed is calculated as a series/parallel combination of the individual resistances for these paths. The advantage of the analytical approach is that it enables one to evaluate easily the relative contributions and trends of each conduction path as a function of the packed bed parameters/properties. Different approaches have been taken by researchers developing analytical models. Some researchers such as Slavin et al. [6] assumed that the contact between two spheres is essentially a point contact and the heat transfer

through the contact region can be ignored for hard materials. Ogniewicz and Yovanovich [7] and Turyk and Yovanovich [8] developed analytical models for predicting the effective thermal conductivity of the basic cells of packed beds of uniformly sized spheres and compared their models with experimental data. Recently Slavin et al. [9] proposed an analytical model which takes into account the effect of radiation and treats random packed beds.

The effect of surface roughness on the thermal conductivity of packed beds has not been addressed in any of the existing analytical models. The objective of this paper is to develop a compact model for predicting the effective thermal conductivity of packed beds of uniformly sized, rough spheres immersed in a stagnant gas at various gas pressures (from atmospheric to vacuum) and subjected to a range of mechanical loads. The trends predicted by the present model allow one to study the effect of important input variables involved in real packed beds. It also provides design tools for predicting and improving the thermal performance of random packed beds. The present model shows good agreement with available SC data, with a relative difference on the order of 7%. The model does not account for tangential (or frictional) forces in the contact area which exist in the FCC arrangement. Thus the model

is not as accurate when compared with FCC data collected by Buonanno et al. [3]. However, it captures the trend of the FCC data of [3] and can be used qualitatively for FCC packing. The data include spheres diameters of 19.05, 25, and 50.4 mm with roughness ranging from 0.03 to 2 μm and rarefied gas pressures.

2. Present model

Modeling the thermal conductivity of spherical packed beds includes two main analyses (i) conduction between rough spheres and (ii) heat transfer through interstitial stagnant gas between solids. The geometry of a general joint is shown in Fig. 1, where two spherical rough caps are placed in mechanical contact. The gap between the contacting bodies is filled with a stagnant gas at pressure P_g and temperature T_g and heat is transferred from one sphere to another. Thermal energy can be transferred across the joint via three distinct modes: radiation, conduction through interstitial gas in the gap, and conduction through the real contact area. Radiation between spheres remains small for most applications of packed beds and can be neglected [10]. Also, natural convection does not occur within the gap between particles when the Grashof number is less than 2500 [11]. In practical situations concerning packed beds, the Grashof number is less than 2500, thus the heat transfer through natural convection is small and can be neglected. Therefore, the remaining heat transfer modes are conduction via the microcontacts and conduction through the interstitial gas filling the gap between contacting bodies.

Heat conduction analysis between contacting rough spheres is the first step toward modeling the thermal conductivity of packed beds. Each cell is made up of contact regions. A contact region is composed of a contact area between two portions of spheres, surrounded by a gas layer. A contact region is the basic element that creates the packed beds. The heat transferred in an isolated contact region determines the thermal behavior of the entire bed. As schematically shown in Fig. 1, conduction occurs through three main paths, the interstitial gas within the microgap Q_g, microcontacts Q_s, and the interstitial gas within the macrogap Q_G. As a result of the small real contact area [12] and low thermal conductivities of interstitial gases, heat flow experiences a relatively large thermal resistance passing through the joint, this phenomenon leads to a relatively high temperature drop across the joint.

The thermal joint resistance of rough spherical surfaces with the presence of an interstitial gas contains four thermal resistance components, (1) the macrocontact constriction/spreading resistance R_L, (2) the microcontacts constriction/spreading resistance R_s, (3) resistance of the interstitial gas in the microgap R_g, and (4) the resistance of interstitial gas in the macrogap R_G, see Fig. 2. As shown, the macrogap provides a parallel path for conduction between the two isothermal planes, therefore the joint resistance can be calculated from

$$R_j = \left[\frac{1}{(1/R_s + 1/R_g)^{-1} + R_L} + \frac{1}{R_G} \right]^{-1} \quad (1)$$

As illustrated in Fig. 2, R_G has three components: the macrogap resistance and the bulk thermal resistance of the solid layers in spheres 1 and 2 (R_1 and R_2), respectively. The solid layers bulk resistances are negligible compared to R_G since the gas thermal conductivity is much smaller than the thermal conductivity of the solids, i.e., $k_g \ll k_s$.

In the following subsections, different thermal resistances in Eq. (1) are discussed and simple correlations are derived for calculating each component.

2.1. Conduction through solid particles

It is assumed that the surface of spheres are randomly rough. When random rough surfaces are placed in mechanical contact, *real* contact occurs at the top of the surface asperities called microcontacts. The real contact area A_r (the summation of the microcontacts) forms a small portion of the nominal contact area, typically less than a few percent of the nominal contact area. The contact between two Gaussian rough surfaces is modeled by the contact between a single Gaussian surface that has the combined
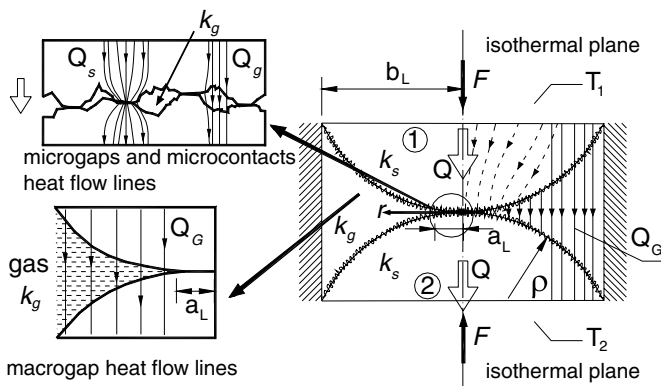

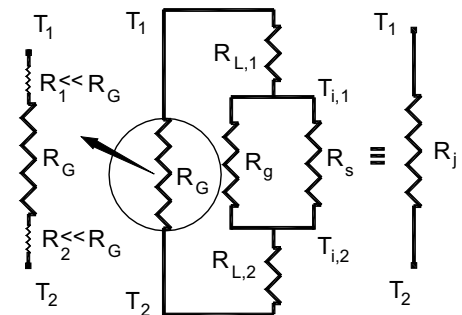Fig. 1. Contact of rough spheres with presence of interstitial gas.

Fig. 2. Thermal resistance network, spherical rough joints in presence of gas.

roughness characteristics of both surfaces with a perfectly smooth surface, for more detail see [13]. The combined roughness σ and surface slope m are $\sigma = \sqrt{\sigma_1^2 + \sigma_2^2}$, $m = \sqrt{m_1^2 + m_2^2}$.

Bahrami et al. [14] developed a compact model to predict the thermal constriction/spreading resistance through the microcontacts, R_s by assuming plastically deformed asperities

$$R_s = \frac{0.565 H^*(\sigma/m)}{k_s F} \qquad (2)$$

With $k_s = 2 k_1 k_2/(k_1 + k_2)$ and $H^* = c_1(\sigma'/m)^{c_2}$, $\sigma' = \sigma/\sigma_0$ and $\sigma_0 = 1$ μm, where c_1 and c_2, are correlation coefficients determined from the Vickers microhardness measurements [10]. Yovanovich and Hegazy [15] showed through experiments that the surface microhardness can be much higher than the bulk hardness and that the microhardness decreases until the bulk hardness is reached. They proposed a correlation for determining the microhardness, $H_{mic} = c_1(d_v/\sigma_0)^{c_2}$, where d_v (μm) is the Vickers indentation diagonal. Sridhar and Yovanovich [16] suggested empirical relations to estimate Vickers microhardness coefficients. Two least-square-cubic fit expressions were reported

$$\begin{aligned} c_1 &= H_{BGM}(4.0 - 5.77\kappa + 4.0\kappa^2 - 0.61\kappa^3) \\ c_2 &= -0.57 + 0.82\kappa - 0.41\kappa^2 + 0.06\kappa^3 \end{aligned} \qquad (3)$$

where $\kappa = H_B/H_{BGM}$, H_B is the Brinell hardness of the bulk material in GPa, and $H_{BGM} = 3.178$ GPa. The above correlations are valid for the range $1.3 \leqslant H_B \leqslant 7.6$ GPa. In situations where an effective value of microhardness H_{mic} is known, the Vickers microhardness coefficients will be $c_1 = H_{mic}$ and $c_2 = 0$.

In a study by Bahrami et al. [17] a general contact pressure distribution was proposed which covers the entire range of spherical rough contacts. This model also covers the limiting case of contact of smooth spheres (Hertzian contact). The following relationships were developed for the maximum contact pressure P_0 and the radius of the macrocontact area a_L [17]

$$P(\xi) = P_0(1 - \xi^2)^\gamma \qquad (4)$$

$$P_0' = \frac{P_0}{P_{0,H}} = \frac{1}{1 + 1.22\alpha\kappa^{-0.16}} \qquad (5)$$

$$\frac{a_L}{a_H} = \begin{cases} 1.605/\sqrt{P_0'}, & 0.01 \leqslant P_0' \leqslant 0.47 \\ 3.51 - 2.51 P_0', & 0.47 \leqslant P_0' \leqslant 1 \end{cases} \qquad (6)$$

where $\xi = r/a_L$, $P_{0,H} = 1.5 F/\pi a_H^2$ and $\gamma = 1.5(P_0/P_{0,H}) \times (a_L/a_H)^2 - 1$. The effective elastic modulus and the equivalent radius of curvature can be found from $1/\rho = 1/\rho_1 + 1/\rho_2$ and $1/E' = (1 - v_1^2)/E_1 + (1 - v_2^2)/E_2$; also $a_H = (0.75 F\rho/E')^{1/3}$ is the Hertzian contact radius. The nondimensional parameters α and κ are defined as

$$\alpha = \frac{\sigma\rho}{a_H^2} \quad \text{and} \quad \kappa = \frac{E'}{H_{mic}}\sqrt{\frac{\rho}{\sigma}} \qquad (7)$$

The proposed model was compared with more than 220 experimental data points collected by others and good agreement was observed [17].

Yovanovich et al. [18] studied the thermal spreading resistance of a heat source on a sphere with different boundary conditions. They showed that for relatively small contact radii, compared to the radius of the sphere, the constriction resistance of the contact region is approximately equal to the constriction resistance of a heat source on a half space. In this study, it is assumed that the macrocontact region is isothermal. Therefore, the macrocontact constriction/spreading resistance is

$$R_L = \frac{1}{2 k_s a_L} \qquad (8)$$

where a_L is calculated using Eq. (6).

2.2. Conduction through gas

Conduction heat transfer in a gas layer between two parallel plates is commonly divided into four heat-flow regimes [19]: continuum, temperature-jump or slip, transition, and free-molecular. The parameter that characterizes the regimes is the Knudsen number, $Kn = \Lambda/d$, where Λ and d are the molecular mean free path and the distance separating the two plates, respectively. The molecular mean free path is defined as the average distance a gas molecule travels before it collides with another gas molecule and it is proportional to the gas temperature and inversely proportional to the gas pressure [20]

$$\Lambda = \frac{P_0}{P_g}\frac{T_g}{T_0}\Lambda_0 \qquad (9)$$

where Λ_0 is the mean free path value at some reference gas temperature and pressure T_0 and P_0. The heat transfer in a gas layer between two isothermal parallel plates at T_1 and T_2 for all four flow regimes can be effectively calculated from [20]

$$q_g = \frac{k_g}{d + M}(T_1 - T_2) \qquad (10)$$

The gas parameter m is defined as

$$M = \left(\frac{2 - \alpha_{T1}}{\alpha_{T1}} + \frac{2 - \alpha_{T2}}{\alpha_{T2}}\right)\left(\frac{2\gamma_g}{1 + \gamma_g}\right)\frac{1}{Pr}\Lambda \qquad (11)$$

where α_{T1}, α_{T2}, γ_g, and Pr are thermal accommodation coefficients corresponding to the gas–solid combination of plates 1 and 2, ratio of the gas specific heats, and gas Prandtl number, respectively. The thermal accommodation coefficient α_T depends on the type of gas–solid combination and is in general sensitive to the condition of the solid surfaces. It represents the degree to which the kinetic energy of a gas molecule is exchanged while in collision with the solid wall. Song and Yovanovich [21] purposed a correlation for estimating α_T for engineering surfaces:

$$\alpha_T = \exp\left[-0.57\left(\frac{T_s - T_0}{T_0}\right)\right]\left(\frac{M^*}{6.8 + M^*}\right)$$
$$+ \frac{2.4\mu}{(1+\mu)^2}\left\{1 - \exp\left[-0.57\left(\frac{T_s - T_0}{T_0}\right)\right]\right\} \quad (12)$$

where

$$M^* = \begin{cases} M & \text{for monatomic gases} \\ 1.4M & \text{for diatomic/polyatomic gases} \end{cases}$$

where $T_0 = 273$ K. Eq. (12) is general and can be used for any combination of gases and solid surfaces for a wide temperature range. The agreement between the predicted values and the experimental data is within 25%. It is worth noting that, these parameters have secondary order effects and slight variations in their values will not have a significant impact on the effective conductivity of the bed.

The authors developed a compact analytical model for predicting the heat conduction through interstitial gas between rough spherical bodies [22]. The non-conforming region between the solids was divided into infinitesimal surface elements where Eq. (10) can be applied. Thermal resistance of the interstitial gas through the microgap and the macrogap were calculated by integrating these surface elements over the macrocontact and the macrogap areas, respectively. The microgap and the macrogap resistances for the contact of two rough spheres can be calculated from [22]

$$R_g = \frac{2\sqrt{2}\sigma a_2}{\pi k_g a_L^2 \ln\left(1 + \frac{a_2}{a_1 + M/(2\sqrt{2}\sigma)}\right)} \quad (13)$$

where $a_1 = \text{erfc}^{-1}(2P_0/H')$ and $a_2 = \text{erfc}^{-1}(0.03P_0/H') - a_1$.

$$R_G = \frac{2}{\pi k_g\left[S\ln\left(\frac{S-B}{S-A}\right) + B - A\right]} \quad (14)$$

where $A = 2\sqrt{\rho^2 - a_L^2}$, $B = 2\sqrt{\rho^2 - b_L^2}$, $S = 2(\rho - \omega_0) + M$, $H' = c_1(1.62\sigma'/m)^{c_2}$, and $\omega_0 = a_L^2/2\rho$. The inverse complementary error function $\text{erfc}^{-1}(x)$ can be found from

$$\text{erfc}^{-1}(x) = \begin{cases} \dfrac{1}{0.218 + 0.735x^{0.173}}, & 10^{-9} \leqslant x \leqslant 0.02 \\[2mm] \dfrac{1.05(0.175)^x}{x^{0.12}}, & 0.02 < x \leqslant 0.5 \\[2mm] \dfrac{1 - x}{0.707 + 0.862x - 0.431x^2}, & 0.5 < x \leqslant 1.9 \end{cases}$$

3. Thermal conductivity of basic cell

The solid fraction ε is the ratio of the solid volume to the total volume of the packed bed, i.e., $\varepsilon = V_s/V$. Consider a basic cell that has the length L_c and the cross sectional area A_c. One dimensional heat conduction is assumed in the basic cell. Thus the top and bottom surfaces are isothermal and the four lateral walls are adiabatic due to symmetry. The applied load is considered as a hydrostatic pressure P_a acting on all the walls. This load can be a result of one or more of the following: the structural load due to the weight of spheres, thermal expansion of the spheres, packing under pressure, exerted external load on the bed, etc.

A real packed bed is a non-homogenous medium of different thermal conductivities corresponding to local variation of apparent load. Depending on this variation, different approaches can be taken to calculate the effective thermal conductivity of the bed. An exact treatment is to integrate the local effective thermal conductivity over the entire bed to find the apparent thermal conductivity. A simpler approach is to consider an average contact load which is constant for all the joints in the bed. This average contact load can be considered as the arithmetic mean between the highest and the lowest contact loads. Later it will be shown that most of the heat transfer occurs through the stagnant gas (macrogap). Changing the contact load will affect the micro and macro thermal resistances, i.e., conduction through particles. The effective thermal conductivity of the bed; however, is not highly sensitive to this change. In addition, when the contact load is introduced, the load linearly increases by increasing the depth in the bed due to the weight of particles. Therefore, the arithmetic mean is an appropriate estimate. In this study the latter method is employed to develop compact expressions for the effective thermal conductivity. However, the first method can also be applied using the same procedure. To evaluate the thermal resistance of the basic cell, the following steps should be taken:

- Calculate the relation between the apparent load on the cell and the contact load on the individual contact. This relation is found from static equilibrium.
- Break up the unit cell into contact regions and find the relation between the cell resistance and the resistance of a contact region.
- Calculate the thermal joint resistance for the contact region and determine the apparent conductivity of the basic cell.

The effective thermal conductivity of the cell can be found by considering a homogenous medium, from: $k_e = L_c/R_cA_c$, where R_c is the resistance of the basic cell.

The boundary resistance R_{BR} arises as a result of the imperfect contact between the spheres and the plates of the container where thermal energy enters and exists the bed. Therefore, the total resistance of the packed bed is $R_{total} = R_{bed} + 2R_{BR}$ where the boundary resistances at both planes are assumed to be identical, see Fig. 4. The total effective thermal conductivity of a packed bed including the boundary resistance can be found from

$$k_{e,total} = \frac{L_{bed}}{A_c(R_{bed} + 2R_{BR})} \quad (15)$$

where $R_{bed} = L_{bed}/(k_eA_c)$ and L_{bed} is the length of the bed in the heat transfer direction. The influence of the

boundary resistance on the effective conductivity of the bed depends on the length of the bed and the diameter of the spheres. The boundary resistance has the same components as the joint resistance discussed in the previous section, see Fig. 2, and Eq. (1) can be used to calculate the boundary resistance. It should be noted that because of the contact geometry of R_{BR}, the effective radius of curvature and the macrogap area are different in R_{BR} than the ones used for the joint resistance between two spheres.

3.1. Simple cubic (SC) packing

The geometry of the SC unit cell is shown in Figs. 1 and 4 where $b_L = \rho$, $A_c = D^2$, $L_c = D$, and $\rho = D/2$. The thermal joint resistance of the cell is determined from Eq. (1) where the components R_s, R_L, R_g, and R_G can be calculated using Eqs. (2), (8), (13), and (14), respectively. The unit cell has one contact region thus $R_c = R_{j,SC}$. The effective thermal resistance of the SC packed beds is

$$k_{e,SC} = \frac{1}{R_{j,SC}D} \qquad (16)$$

Kitscha and Yovanovich [23] conducted experiments and investigated the solid and gas conduction for a contact between a sphere and a rough flat. The load on the contact was varied to study the effect of the applied load on the solid and gas conduction. For each load (or contact size) the gas pressure was varied from vacuum to atmospheric conditions. Two gases were used, air and argon, to study the effect of gas properties on the gas conduction. Two spherical carbon steel samples of radii 12.7 and 25.4 mm were chosen. The flat specimen was a steel 1020 with the roughness of $\sigma = 0.13\,\mu m$ and an effective microhardness $H_{mic} = 4$ GPa. Specimens were cylindrical with the same radius, $b_L = 12.7$ mm. To minimize the radiation and convection heat transfer to the surroundings, the lateral surfaces of the specimens were insulated. Tests were conducted in a 70–90 °C temperature range. Fig. 3a–c illustrates the comparison between the present model and Kitscha and Yovanovich [23] data. The data show good agreement with the model with a relative RMS difference of approximately 7.2%.

Buonanno et al. [3] conducted experiments and measured the effective thermal conductivity of rough spherical packed beds. They tested beds of uniform sphere size which were packed in the SC and FCC arrangements. The spheres were stainless steel $100Cr_6$ of diameter 19.05 mm. Buonanno et al. [3] performed four tests with different surface roughness for each packing. The combined RMS surface roughness was varied from 0.03 to 1.7 μm. Their experimental apparatus and its properties are described in Fig. 4. Thermal energy enters the packed bed at the top copper plate and leaves the system at the bottom copper plate, two flux meters were used to measure the heat flow to the bed. The lateral sides of the bed were insulated to insure one-dimensional heat transfer. They reported an average contact load for each packing, which was the arith-
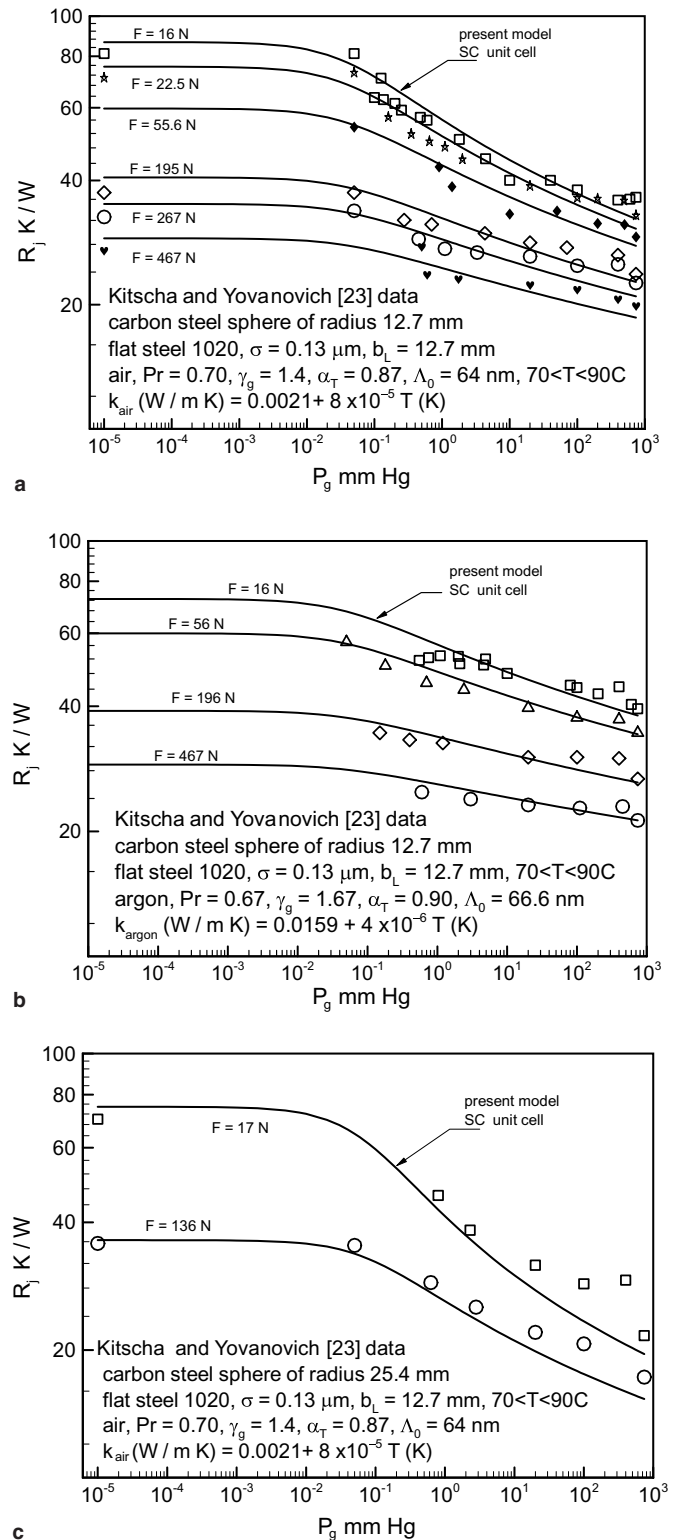
Fig. 3. Comparison of model with Kitscha and Yovanovich [23] SC data.

metic mean of the structural weight of the spheres. Buonanno et al. [3] measured the total effective thermal conductivity of the bed which included the boundary thermal resistance R_{BR} at the top and bottom copper plates. To compare the present model with Buonanno et al.'s data [3],
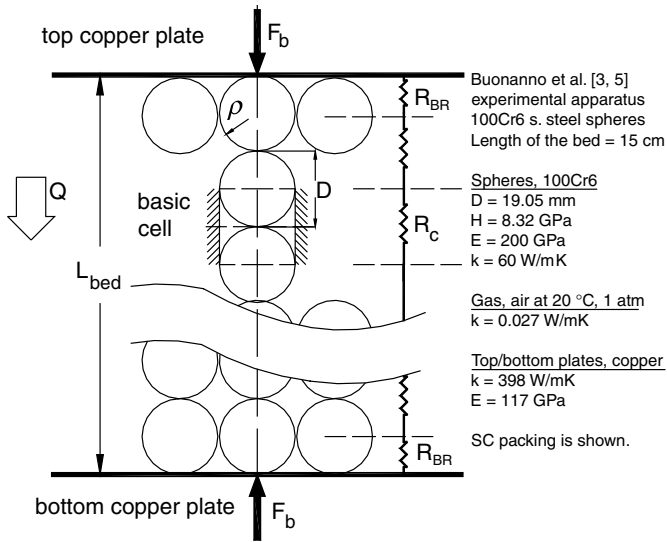
Fig. 4. Buonanno et al. [3,5] experimental apparatus for SC packing.

the total thermal resistance of their packed bed is calculated using Eq. (15) where the average contact load reported as 0.983 N is used. The comparison between the present model and Buonanno et al. [3] data is shown in Fig. 5a.

Buonanno et al. [5] using the same experimental apparatus described in Fig. 4, conducted experiments to study the effect of applied load on the effective thermal conductivity of packed beds. They reported the contact loads for two levels of combined surface roughness of 0.03 and 1.7 μm, without describing the method of applying the external load. The present model is compared with the reported data of [5] in Fig. 5b. As shown both data sets show good agreement with the present model.

All thermophysical, mechanical, and surface properties shown in the comparisons are the values reported by researchers; Buonanno et al. [3,5], and Kitscha and Yovanovich [23].

3.2. Face centered cubic (FCC) packing cell

The FCC packing contact region is shown in Fig. 6 where two 1/8 spheres make contact with $L_c = \sqrt{2}D/2$ and $A_c = D^2/2$. From symmetry, contact loads are identical. It is assumed that there are no frictional or tangential forces in contact regions. For the FCC contact, the basic cell thermal resistance components, R_s, R_L, R_g can be calculated using Eqs. (2), (8), and (13), respectively. Since the thermal conductivity of solids are much larger than the gas thermal conductivity, the sphere surfaces can be assumed as isotherms. Also, the top and the bottom plates of the cell are isotherms. Therefore, the problem is reduced to finding the thermal resistance between these isotherms. There are two parallel paths for conduction in the FCC macrogap. The first path is the heat transfer between two spheres, indicated by Q_1, in which Eq. (14) can be used with $b_L = \rho \tan \varphi$ to calculate R_{G1}. The angle φ is estimated
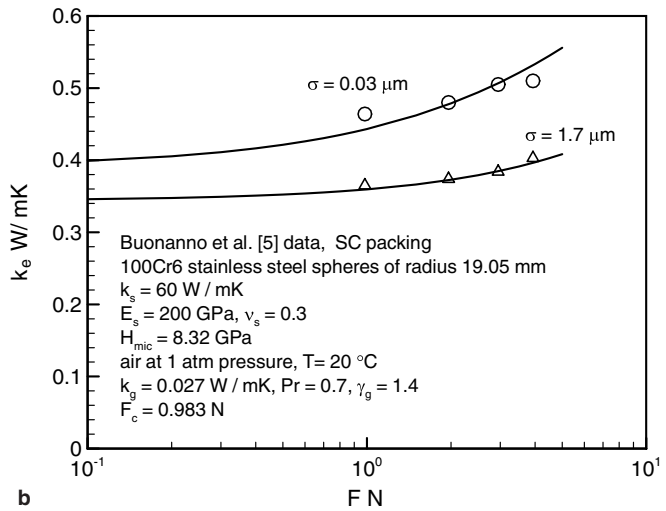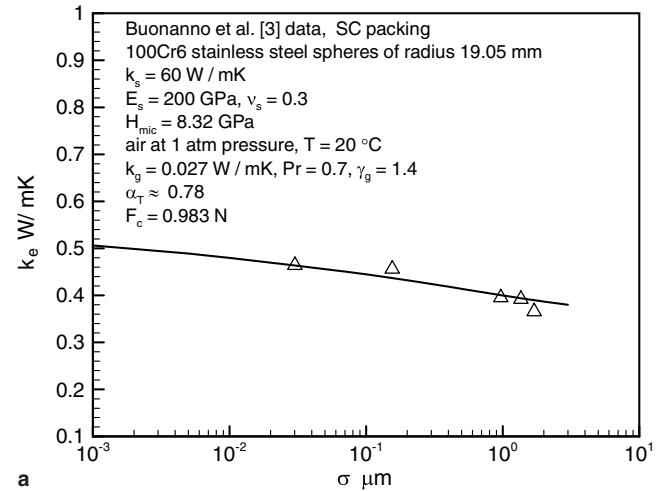
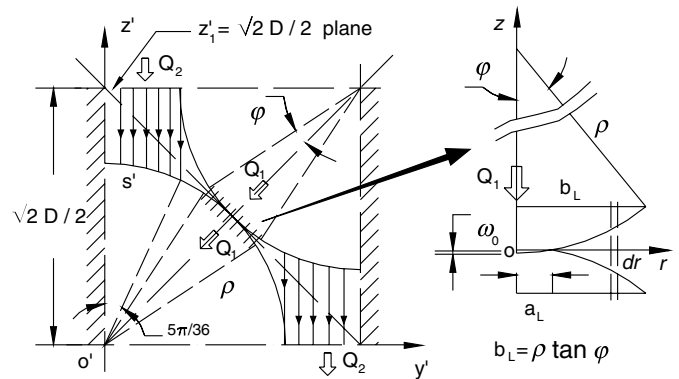Fig. 5. Comparison of present model with Buonanno et al. [3,5] SC data.

Fig. 6. FCC contact region, heat transfer paths in macrogap.

(arbitrarily) to be 10° or π/18 by considering the flow lines between two spheres, see Fig. 6. Note that the result of the analysis is not significantly sensitive to the value of the angle φ. The second path is the heat transfer between the isothermal plane $z'_1 = \sqrt{2}D/2$ and the isothermal sphere $s' = \rho \cos \phi$, indicated by Q_2, which can be found from

$$Q_2 = \int\int \frac{k_g \Delta T \cos\phi \, dA}{z_1' - s' + M} \tag{17}$$

where $dA = \rho^2 \sin\phi \, d\phi \, d\theta$ is a surface element on the sphere s', where $0 \leqslant \phi \leqslant 5\pi/36$, and $-\pi/4 \leqslant \theta \leqslant \pi/4$. Therefore, the thermal resistance for path Q_2 is

$$R_{G2} = \frac{1}{\pi k_g \rho \left[B \ln\left(\frac{B-0.9036}{B-1}\right) - 0.09369 \right]} \tag{18}$$

where $B = \sqrt{2} + M/\rho$. The heat transfer area corresponding to the path Q_1, a circle of radius b_L, is relatively small compared to the sphere surface area. This adds a constriction/spreading to the path Q_1 which can be estimated using Eq. (8), i.e., $1/(2k_s b_L)$. Therefore, the macrogap thermal resistance for FCC is

$$\frac{1}{R_{G,FCC}} = \frac{1}{1/(2k_s b_L) + R_{G1}} + \frac{1}{R_{G2}} \tag{19}$$

Due to the relatively small gas layer thickness, most of the heat transfer occurs through the path Q_1; in other words $R_{G2} \gg R_{G1}$ thus Q_2 may be neglected with respect to Q_1. The macrogap thermal resistance for the FCC contact can be simplified to, $R_{G,FCC} = R_{G1} + 1/(2k_s b_L)$. The thermal contact resistance for a FCC contact region can be found from Eq. (1). There are four parallel half-contact regions in the FCC unit cell. Thus, the thermal resistance of the unit cell is half of a FCC contact region, $R_c = R_{j,FCC}/2$. It should be noted that each 1/8 sphere contains only half of the contact region (or double the constriction/spreading resistance), thus a factor of 2 must be considered. The effective thermal resistance for FCC packed beds is

$$k_{e,FCC} = \frac{2\sqrt{2}}{R_{j,FCC} D} \tag{20}$$

The total effective thermal conductivity of the FCC bed, including boundary resistance, can be calculated using Eq. (15).

Buonanno et al. [3] measured the apparent conductivity of FCC packed beds with four levels of roughness and reported an average contact load (normal) without considering the effect of tangential/frictional forces in the contact area. The reported mean contact load was the mean structural weight of their FCC packed bed, $F_c = 0.78$ N. Of course, the real normal contact loads in the bed could not be measured directly. Due to the frictional/tangential forces in the FCC contact area, normal loads which determine the macrocontact area, will be smaller than the reported value. As for the SC arrangement, the effect of frictional/tangential forces is small and therefore can be neglected.

The contact mechanics of the present model do not account for tangential forces in the contact area corresponding to the friction between the contacting spheres. Considering the effect of friction on the contact load is a complex task and requires knowledge of the friction factor(s) between the spheres in the packed bed. Therefore, a quantitative comparison between the present model and

the FCC data of [3] is impossible. However, a qualitative comparison which shows the trends of the model and the data is presented in Fig. 7a. Two curves are shown for the model. The dashed line in which the reported contact load is used, i.e., $F_c = 0.78$ N. The solid curve represents the model in which an arbitrary constant factor of 0.5 is applied to the reported contact load to account for the friction between spheres. As expected, the difference between the data and the model is larger at higher roughness values which indicates that the effect of friction is more significant at higher roughness values.

The present model is also compared with Buonanno et al. data [5] where the effect of contact load on the effective thermal conductivity was experimentally investigated. Two sets of data were collected for two levels of combined surface roughness, i.e., 0.03 and 1.7 μm as the applied load was varied [5]. As discussed above, two constants were considered on the reported contact loads to account for the effect of the tangential/frictional forces on the macrocontact, i.e., 0.8 and 0.5 for 0.03 and 1.7 μm surface roughness
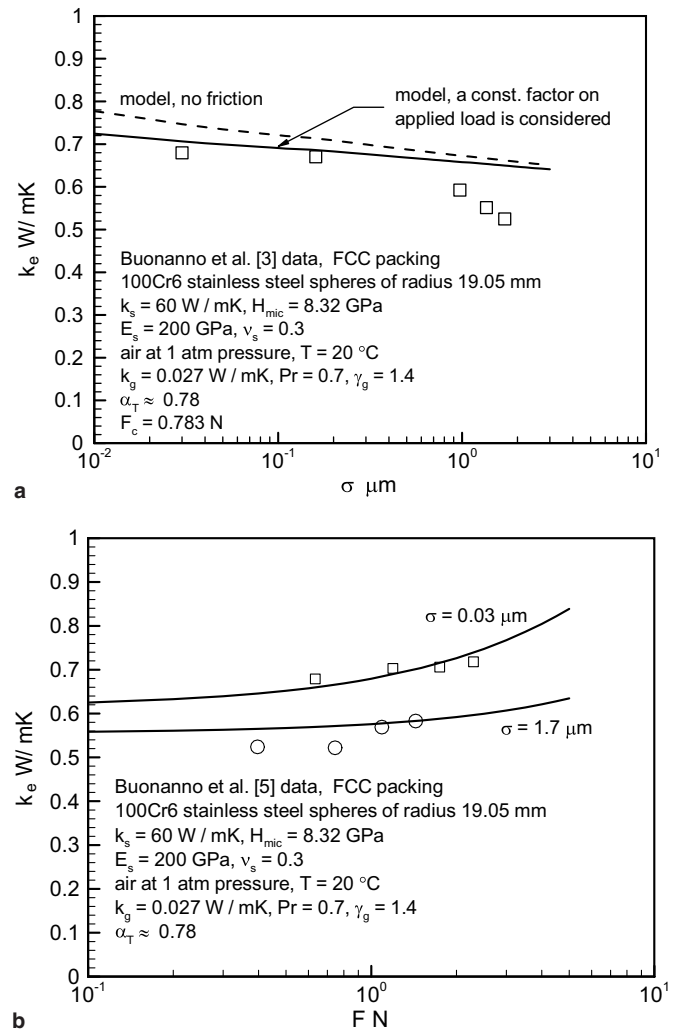
Fig. 7. Comparison of present model with Buonanno et al. [5] data, FCC packing.

data, respectively. As shown in Fig. 7a and b, the model shows the trend of the data. It also can be concluded that the effect of frictional forces in FCC packing becomes more important as the surface roughness increases.

4. Parametric study

The proposed model can be used to investigate the influence of important parameters/properties of a packed bed on its effective thermal conductivity. The effects of roughness and applied load on effective conductivity for both SC and FCC packings have been investigated in the previous section. In this section, the effect of the gas and its pressure, the relative size of spheres, and the thermal conductivity of spheres on the effective thermal conductivity of bed are investigated. Since the trends of both SC and FCC packings are similar, only the SC packing results are presented.

The influence of roughness on the SC joint resistance and its components predicted by the model is shown in Fig. 8. The same input parameters/properties of the SC packed bed of [3] is used, see Fig. 4. As roughness is increased, while other contact parameters listed in Fig. 8 are held constant, it can be seen that (i) the microcontacts resistance R_s increases linearly, see Eq. (2), (ii) the contact load spreads over a larger area or the macrocontact area increases which leads to a lower macrocontact resistance R_L, (iii) as a result of larger macrocontact area, the macrogap area becomes smaller thus the macrogap resistance R_G becomes higher (slightly in this case); also it can be observed that most of the heat transfer occurs through the macrogap, and (iv) the microgap resistance R_g is very high and can be neglected. Another interesting trend can be observed in the microgap resistance R_g. As roughness decreases, the separation between two spheres in the macrocontact area decreases, i.e., the size of the microgaps becomes smaller, see Fig. 1, which has a decreasing effect

on R_g. Also with smaller microgaps, the rarefaction effect in the microgaps becomes more important which leads to an increase in the microgap resistance R_g. As a result of these two competing effects, the microgap resistance R_g decreases to a certain point and then approaches its limit where roughness is zero, as shown in Fig. 8. This limit can be found from Eq. (13)

$$\lim_{\sigma \to 0} R_g = \frac{M}{\pi k_g a_H^2} \tag{21}$$

It should be noted that for smooth surfaces the microcontacts resistance $R_s = 0$ and since R_s and R_g are in parallel, Eq. (1), the value of R_g does not change the joint resistance.

Fig. 9 illustrates the effect of the interstitial gas type and its pressure on the effective thermal conductivity of the same packed bed described above, with a surface roughness $\sigma = 0.5\ \mu m$. Two different gases, air and helium, are chosen for the comparison since their thermal conductivities differ greatly, i.e., 0.026 and 0.153 W/m K, respectively. For each gas the gas pressure is varied from vacuum (approximately 10^{-5} Torr) to atmospheric pressure 760 Torr, see Fig. 9 for the bed and gases properties. It can be seen that in a vacuum and very low gas pressures thermal conductivities of both beds are identical. As expected, with increasing gas pressure the bed filled with helium shows higher effective conductivity, a factor of 4.7 higher at atmospheric pressure.

The variation of the effective thermal conductivity of a SC packed bed, the same bed as described above, versus the relative diameter of spheres D/L_{bed} is presented in Fig. 10. The average contact load for each sphere diameter value is considered as half of the weight of a column of spheres in a packed bed of 150 mm length and the density of $100Cr_6$ spheres is assumed to be 7800 kg/m³. All other input parameters are held constant as the diameter of spheres is varied over the range of $0.1 \leqslant D \leqslant 75$ mm, i.e., $0.0007 \leqslant D/L_{bed} \leqslant 0.5$, see Fig. 10 for other input
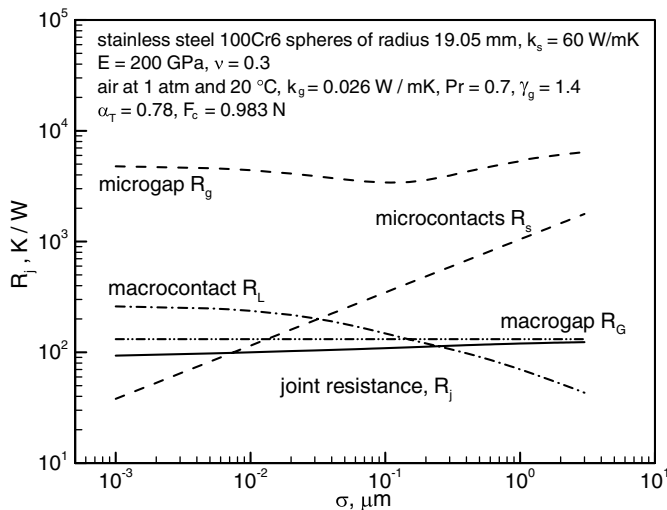

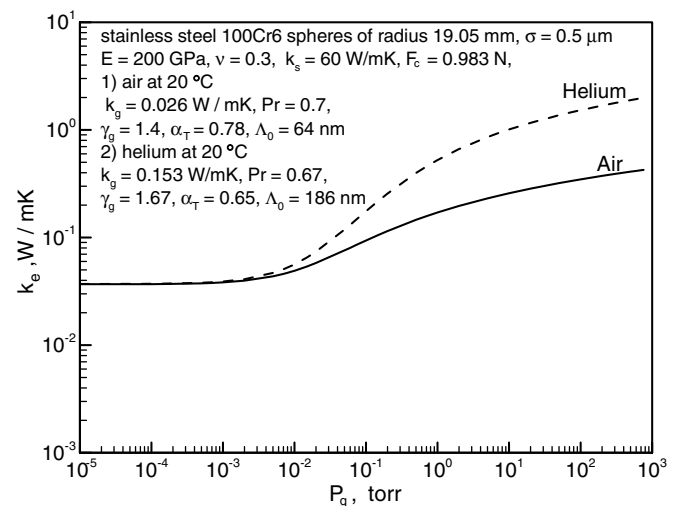Fig. 8. Effect of roughness on joint resistance and ITS components, SC contact region.

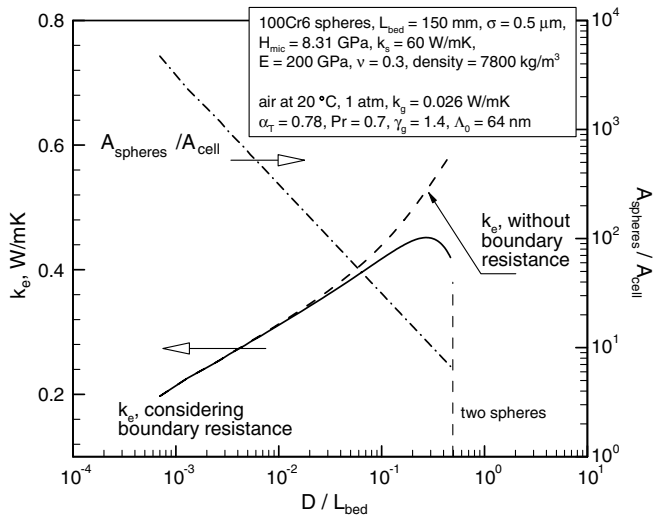Fig. 9. Effect of gas type and pressure on effective thermal conductivity of SC arrangement.

Fig. 10. Effect of particle radius on effective thermal conductivity of SC packed beds.

Fig. 11. Effect of spheres thermal conductivity on effective conductivity of SC arrangement.

parameters. As shown, the effective thermal conductivity increases as the diameter of the spheres increases. This is a direct result of decreasing the total relative surface area of the spheres in the packed bed $A_{spheres}/A_{cell}$ and increasing the mean contact load. In addition, the variation of the ratio $A_{spheres}/A_{cell}$ as a function of the relative size of the spheres is shown in Fig. 10.

The effect of boundary resistance on the effective thermal conductivity of the bed is also shown in Fig. 10. The boundary resistance is calculated as discussed in Eq. (15). Two curves are shown in the plot, the boundary resistance is considered in calculating the solid curve and it is neglected in the dashed curve. As shown, the effect of the boundary resistance is relatively small when the relative size of the spheres is small.

Fig. 11 presents the effect of the thermal conductivity of spheres on the effective conductivity of a bed. As the conductivity of the spheres is increased, while other parameters listed in Fig. 11 are held constant, one can observe: (i) the effective conductivity of the bed is a weak function of the conductivity of the spheres. By increasing the conductivity of the spheres up to 1000 W/m K, the effective conductivity of the bed increases only up to approximately 5 W/m K. (ii) In a vacuum, a linear relationship exists between the thermal conductivity of the bed and the particle thermal conductivity, (iii) Most of the heat transfer occurs through the gas. By increasing the gas pressure from vacuum to 0.1 mmHg (even though it is still a partial vacuum) a relatively large increase in the packed bed thermal conductivity is seen. (iv) At higher particle thermal conductivity (1000 W/m K), the effect of gas pressure becomes negligible, i.e., the effective conductivity of the bed approaches that of the vacuum condition. In other words, most of the heat transfer occurs through the particles. It is interesting to note that the vacuum condition serves as a limit where the spheres conductivity approaches infinity.
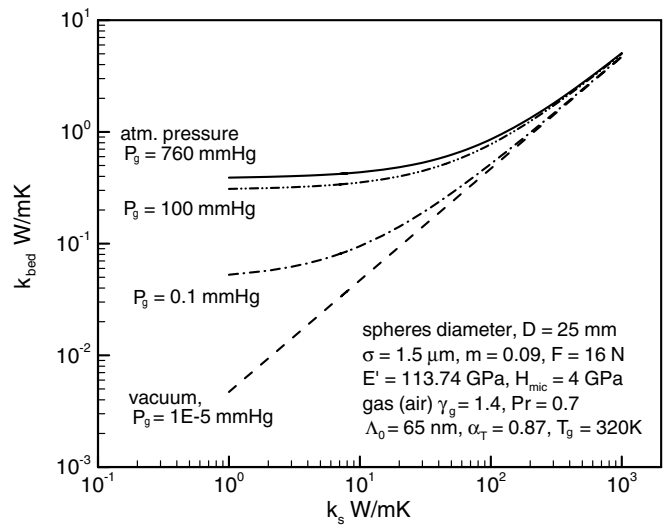
5. Summary and conclusions

Analytical solutions for steady-state conduction heat transfer in regularly packed beds of rough spheres with a uniform diameter in the presence of a stagnant gas are developed. SC and FCC packing are studied since they present the upper and lower bounds for the effective thermal conductivity of randomly packed beds. Compact relationships are derived for calculating the effective thermal conductivities of SC and FCC unit cells. These models account for the thermophysical properties of spheres and the gas, contact load, spheres diameter, spheres roughness and surface asperity slope, and temperature and pressure of the stagnant gas. The present model is compared against both "basic cell" and "packed bed" data for a wide range of parameters including: gas pressure and temperature, gas type, contact load, particle size, and surface conditions.

Experimental data of [23] collected for SC basic cells are compared with the model. The data are collected at different applied loads where at each load the gas pressure is varied from vacuum to atmospheric pressure. Experiments include two diameters of stainless steel spheres with argon and air as interstitial gas. The present model shows good agreement with the data of [23] with the RMS difference in the order of 7%.

The present model is also compared with experimental data collected by Buonanno et al. [3,5] for SC and FCC regularly packed beds and showed good agreement with SC data. Due to the frictional/tangential forces in the FCC contact region, the present model can not be compared quantitatively with the FCC data. However, the model shows the trend of the FCC data in a qualitative comparison. The data include a range of the contact load and the surface roughness of the single-sized stainless steel spheres in air at atmospheric condition.

The influence of the surface roughness on the joint resistance predicted by the model and its components are

presented and their trends are discussed. It is shown that most of the heat transfer occurs through the gas in the macrogap when the thermal conductivity of particles are not "too high". Effects of the gas type, gas pressure, and the relative size of the spheres on the effective thermal conductivity of the beds are studied. It is observed that the thermal conductivity of packed beds increase by increasing the relative diameter of the spheres. Moreover, the effective thermal conductivity of packed beds is a weak function of the thermal conductivity of spheres. It is also shown that the vacuum condition serves as a limit where the spheres conductivity approaches infinity. The influence of the boundary resistance on the conductivity of packed beds is investigated. It is shown that for an uncompressed packed bed, the effect of boundary resistance is negligible where the ratio of the spheres diameter over the bed length is approximately 0.02.

Acknowledgments

References

[1] S. Kikuchi, T. Kuroda, M. Enoeda, Preliminary thermo-mechanical analysis of ITER breeding blanket, JAERI Tech. (1999) 98058.

[2] C.L. Tien, K. Vafai, Statistical bounds for the effective thermal conductivity of microsphere and fibrous insulation, AIAA Prog. Ser. 65 (1979) 135–148.

[3] G. Buonanno, A. Carotenuto, G. Giovinco, N. Massarotti, Experimental and theoretical modeling of the effective thermal conductivity of rough steel spheroid packed beds, J. Heat Transfer, ASME 125 (2003) 693–702.

[4] G. Buonanno, A. Carotenuto, The effective thermal conductivity of packed beds of spheres for a finite contact area, Numer. Heat Transfer 37 (2000) 343–357.

[5] G. Buonanno, A. Carotenuto, G. Giovinco, N. Massarotti, Effective thermal conductivity of rough spheres packed beds, in: Proceedings of HT2003, ASME Heat Transfer Conference, July 21–23, Las Vegas, NV, USA, Paper No. HT2003-47130, 2003.

[6] A.J. Slavin, F.A. Londry, J. Harrison, A new model for the effective thermal conductivity of packed beds of solid spheroids: alumina in helium between 100 and 500 °C, J. Heat Mass Transfer 43 (2000) 2059–2073.

[7] Y. Ogniewicz, M.M. Yovanovich, Effective conductivity of regularly packed spheres: basic cell model with constriction, in: L.S. Fletcher (Ed.), Heat Transfer and Thermal Control Systems, Progress in Astronautics and Aeronautics, vol. 60, AIAA, New York, 1978.

[8] P.J. Turyk, M.M. Yovanovich, Modified effective conductivity models for basic cells of simple cubic packed beds, in: Proc. 23rd National Heat Transfer Conference, August 4–7, Denver, Colorado, HTD, vol. 46, 1984, pp. 9–19.

[9] A.J. Slavin, V. Arcas, C.A. Greenhalgh, E.R. Irvine, D.B. Marshall, Theoretical model for the thermal conductivity of a packed bed of solid spheroids in the presence of a static gas, with no adjustable parameters except at low pressure and temperature, J. Heat Mass Transfer 45 (2002) 4151–4161.

[10] M.M. Yovanovich, E.E. Marotta, Thermal spreading and contact resistances, in: A. Bejan, D. Kraus (Eds.), Heat Transfer Handbook, John Wiley and Sons Inc., Hoboken, New York, USA, 2003 (Chapter 4).

[11] V.S. Arpaci, P.S. Larsen, Convection Heat Transfer, Prentice-Hall Inc., Englewood Cliffs, NJ 07632, USA, 1984 (Chapter 4).

[12] J.A. Greenwood, J.H. Tripp, The elastic contact of rough spheres, ASME: J. Appl. Mech. 89 (1) (1967) 153–159.

[13] M. Bahrami, J.R. Culham, M.M. Yovanovich, G.E. Schneider, Review of thermal joint resistance models for non-conforming rough surfaces in a vacuum, ASME J. Appl. Mech. Rev. 59 (2006) 1–12.

[14] M. Bahrami, J.R. Culham, M.M. Yovanovich, Thermal contact resistance: a scale analysis approach, ASME J. Heat Transfer 126 (2004) 896–905.

[15] M.M. Yovanovich, A. Hegazy, An accurate universal contact conductance correlation for conforming rough surfaces with different micro-hardness profiles, AIAA, Paper No. 83-1434, 1983.

[16] M.R. Sridhar, M. Yovanovich, Empirical methods to predict Vickers microhardness, Wear 193 (1996) 91–98.

[17] M. Bahrami, M.M. Yovanovich, J.R. Culham, A compact model for spherical rough contacts, ASME J. Tribol. 127 (2005) 884–889.

[18] M.M. Yovanovich, G.E. Schneider, C.H. Tien, Thermal resistance of hollow spheres subjected to arbitrary flux over their poles, Paper No. 78-872, 2nd AIAA/ASME Thermophysics and Heat Transfer Conference, May 24–26, Palo Alto, CA, 1978.

[19] G.S. Springer, Heat transfer in rarefied gases, in: T.F. Irvine, J.P. Hartnett (Eds.), Advances in Heat Transfer, vol. 7, 1971, pp. 163–218.

[20] E.H. Kennard, Kinetic Theory of Gases, McGraw-Hill, New York, London, 1938.

[21] S. Song, M.M. Yovanovich, Correlation of thermal accommodation coefficient for engineering surfaces, in: National Heat Transfer Conference, Pittsburgh, PA, August 9–12, 1987.

[22] M. Bahrami, J.R. Culham, M.M. Yovanovich, Thermal joint resistance of non-conforming rough surfaces with gas-filled gaps, AIAA J. Thermophys. Heat Transfer 18 (2004) 326–332.

[23] W.W. Kitscha, M.M. Yovanovich, Experimental investigation on the overall thermal resistance of sphere-flat contacts, Progress in Astronautics and Aeronautics: Heat Transfer with Thermal Control Applications, vol. 39, p. 93, Also AIAA paper 74-13, 1974.